

Hydrogen isotopic replacement and microstructure evolution in zirconium deuteride implanted by 150 keV protons

Man Zhao(赵嫚), Mingxu Zhang(张明旭), Tao Wang(王韬), Jiangtao Zhao(赵江涛), Pan Dong(董攀), Zhen Yang(杨振), and Tieshan Wang(王铁山)

Citation: Chin. Phys. B, 2021, 30 (**10**): 106104. DOI: 10.1088/1674-1056/ac29a7
Journal homepage: http://cpb.iphy.ac.cn; http://iopscience.iop.org/cpb

What follows is a list of articles you may be interested in

Microstructure evolution of T91 steel after heavy ion irradiation at 550 ℃

Ligang Song(宋力刚), Bo Huang(黄波), Jianghua Li(李江华), Xianfeng Ma(马显锋), Yang Li(李阳), Zehua Fang(方泽华), Min Liu(刘敏), Jishen Jiang(蒋季伸), and Yanying Hu(胡琰莹)
Chin. Phys. B, 2021, 30 (**8**): 086103. DOI: 10.1088/1674-1056/ac0a64

Effect of tellurium (Te^{4+}) irradiation on microstructure and associated irradiation-induced hardening

Hefei Huang(黄鹤飞), Jizhao Liu(刘继召), Guanhong Lei(雷冠虹), Ondrej Muránsky, Tao Wei, and Mihail Ionescu
Chin. Phys. B, 2021, 30 (**5**): 056108. DOI: 10.1088/1674-1056/abf039

Effect of thermo-mechanical process on structure and high temperature shape memory properties of Ti-15Ta-15Zr alloy

Xiao-Hang Zheng(郑晓航), Jie-He Sui(隋解和), Zhe-Yi Yang(杨哲一), Guo-Zhang Zhi(张治国), Wei Cai(蔡伟)
Chin. Phys. B, 2017, 26 (**5**): 056103. DOI: 10.1088/1674-1056/26/5/056103

Microstructure evolution of Cu atomic islands on liquid surfaces in the ambient atmosphere

Zhang Xiao-Fei, Chen Hang, Yu Sen-Jiang
Chin. Phys. B, 2015, 24 (**7**): 076103. DOI: 10.1088/1674-1056/24/7/076103

Small-angle X-ray analysis of the effect of grain size on the thermal damage of octahydro-1, 3, 5, 7-tetranitro-1, 3, 5, 7 tetrazocine-based plastic-bounded expolsives

Yan Guan-Yun, Tian Qiang, Liu Jia-Hui, Chen Bo, Sun Guang-Ai, Huang Ming, Li Xiu-Hong
Chin. Phys. B, 2014, 23 (**7**): 076101. DOI: 10.1088/1674-1056/23/7/076101

SPECIAL TOPIC — Ion beam modification of materials and applications

Hydrogen isotopic replacement and microstructure evolution in zirconium deuteride implanted by 150 keV protons*

Man Zhao(赵嫚)[1], Mingxu Zhang(张明旭)[1], Tao Wang(王韬)[2,†], Jiangtao Zhao(赵江涛)[1], Pan Dong(董攀)[2], Zhen Yang(杨振)[3], and Tieshan Wang(王铁山)[1,‡]

[1] *School of Nuclear Science and Technology, Lanzhou University, Lanzhou* 730000, *China*
[2] *Institute of Fluid Physics, CAEP, Mianyang* 621900, *China*
[3] *Sino–French Institute of Nuclear Engineering and Technology, Sun Yat-Sen University, Zhuhai* 519082, *China*

(Received 15 June 2021; revised manuscript received 15 September 2021; accepted manuscript online 24 September 2021)

Zirconium tritiated (ZrT_x) is an alternative target material for deuteron–triton (D-T) reaction neutron generator. The isotopic replacement and microstructure evolution induced by hydrogen isotope implantation could significantly affect the performance of the target film. In this work, the zirconium deuteride film deposited on Mo/Si substrate was implanted by 150 keV protons with fluence from 1×10^{16} to 1×10^{18} protons/cm^2. After implantation, the depth profiles of retained hydrogen (H) and deuterium (D) in these target films were analyzed by elastic recoil detection analysis (ERDA), and time of flight-secondary ion mass spectrometry (ToF-SIMS). Additionally, the microstructure evolution was also observed by x-ray diffraction (XRD) and scanning electron microscope (SEM). The D concentration in the ZrD_x film decreased versus the proton implantation fluence. An analytical model was proposed to describe the hydrogen isotopic trapping and exchange as functions of incident protons fluence. Additionally, the XRD analysis revealed that no new phase was formed after proton implantation. Furthermore, circular flakings were observed on the ZrD_x surface from SEM images at fluence up to 1×10^{18} protons/cm^2, and this surface morphology was considered to associate with the hydrogen atoms congregation in Mo/Si boundary.

Keywords: zirconium deuterides, isotopic replacement, proton implantation, microstructure evolution

PACS: 61.80.–x, 85.40.Ry, 61.82.Bg **DOI:** 10.1088/1674-1056/ac29a7

1. Introduction

A neutron generator based on the deuteron–triton (D-T) reaction has many applications in measurement cross-section for nuclear reactions, fusion reactor material irradiation, neutron activation analysis, and other industry fields.[1–3] The tritiated metallic film where the D-T reaction occurs is one of the important components of a neutron generator.[4,5] In recent years, zirconium tritiated (ZrT_x) is chosen as a candidate material for the target film because of the excellent hydrogen storage properties[6,7] and higher thermal stability than titanium tritiated (TiT_x).[8,9] However, the neutron beam flux and duration are influenced by the target film properties during D ions implantation. It is known that tritium replacement by implanted deuterons will result in the decrease of tritium concentration which reduces the intensity of the 14 MeV neutron.[10,11] Furthermore, the D ions implantation can significantly influence the integrity of structural components with the formation of voids, surface swelling, blistering and even crack, exfoliation in the tritium target.[12–15] Thus, the knowledge of the hydrogen isotopes effect and the microstructural changes of the target, is of essential importance for the assessment of the target lifetime.

In the previous studies, Doyle and Blewer have observed the exchange of hydrogen isotopes in titanium compounds and established several models to explain.[16–18] Hughey *et al.* have also discussed the physical mechanisms of tritium replacement by implanted deuterons.[11] Further, Karamanis *et al.* have conceived a collisional displacement model to explain tritium release from TiT_x target.[19] Many attempts have also been made to investigate the effects of hydrogen isotopes irradiation on the target structure.[20,21] Yang and Liu *et al.* have observed the cracking feature and phase transformation of titanium hydride film under irradiation of energy density close to 0.5 J/cm^2.[22] Astrelin *et al.*[23] have investigated the blistering process on the surfaces of long-lifetime neutron-generating targets irradiated by an intense 200 keV proton beam. However, there were no sufficient studies on the interaction between hydrogen isotopes and ZrT_x implanted with massive D ions, especially the isotopic exchange and hydrogen damage in this new kind of target film candidate.

Deuterium and tritium, as two different isotopes of hydrogen, have similar chemical properties. Therefore, the properties of the tritium target were often studied by proton implantation to avoid neutron generation.[11,23,24] In this work, the

*Project supported by the National Natural Science Foundation of China (Grant Nos. 11905206 and 11975217).
†Corresponding author. E-mail: wangtaoxtc@gmail.com
‡Corresponding author. E-mail: tswang@lzu.edu.cn
© 2021 Chinese Physical Society and IOP Publishing Ltd

phenomena of isotopic replacement and microstructure evolution in ZrD_x under 150 keV protons implantation were studied instead of ZrT_x target irradiated by deuterium ions. The depth profiles of retained H and D in the zirconium deuteride film were obtained by elastically recoil detection analysis (ERDA) combined with time of flight-secondary ion mass spectrometry (ToF-SIMS), which is one of the most useful methods to evaluate the concentration of hydrogen isotopes in materials. An analytical model was proposed to analyze the experimental data. Furthermore, the x-ray diffraction (XRD) analysis and scanning electron microscope (SEM)/energy dispersive x-ray spectroscopy (EDS) were conducted to understand the microstructure variation induced by proton implantation.

2. Experiment

2.1. Preparation of ZrD_x films

Molybdenum (Mo) film with a thickness of about 0.5 μm was deposited on the polished silicon substrate by magnetron sputtering method as diffusion suppression layer. Then, this Mo film with Si substrate was rinsed with mixed acid (nitric acid and sulfuric acid) and washed in deionized water subsequently. To remove surface contamination, the film was cleaned with acetone in the ultrasonic cleaner for 30 minutes and dried under a nitrogen atmosphere. After that, the ZrD_x film ($\sim$ 3.4 μm) was grown on the molybdenum layer by one-step reactive magnetron sputtering at 573 K substrate temperature and 250 V DC substrate bias. High purity argon (99.999%) gas and deuterium (99.999%) gas were used as the sputtering gas and reactive gas, respectively. A metallic Zr target of high purity (99.95%) was utilized as sputtering targets to deposit the ZrD_x films. The base pressure was about 10^{-5} Pa. The total pressure of the (Ar+D_2) gas mixture was set at 0.4 Pa, while the rate of Ar flow and D_2 flow was 10 SCCM and 20 SCCM, respectively.

2.2. Proton implantation

For proton implantation experiments, the samples were mounted on a sample holder with a conductive adhesive tab in the chamber at the 400 keV ion implanter (NEC Corporation) of Xiamen University. They were exposed to 150 keV protons beams with the different fluence of 1×10^{16}, 3×10^{16}, 1×10^{17}, and 1×10^{18} protons/cm^2. A proton beam with a current below 50 μA/cm^2 was implanted to all specimens at an angle of 90° against the target specimen under high vacuum conditions. The chamber vacuum of 5×10^{-4} Pa can generally be achieved by using molecular pumps during ion beam implantation. The proton beam was raster scanned over each specimen to produce uniform damage during the irradiation. The temperature of the sample holder was controlled at room temperature (RT) by a water cooling system as continuously monitored by a thermocouple placed near the sample.

As presented in Fig. 1, the displacement damage and protons deposition distribution profile of 150 keV proton beam implantation at the fluence of 1×10^{18} protons/cm^2 have been calculated by SRIM-2008. It can be clearly seen that the maximum penetration depth of 150 keV protons in ZrD_x film is $\sim$ 855 nm and the maximum damage values at the Bragg peak position are calculated to be $\sim$ 3.6 dpa.

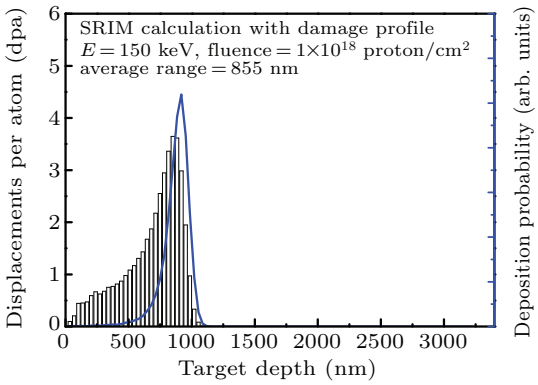


Fig. 1. The depth-dependent damage distribution and protons deposition peak of 150 V proton calculated by SRIM results.

2.3. Characterization methods

The H and D concentrations within the near-surface layer (about $\sim$ 0.3 μm) were measured by ERDA using at 1.95 MeV helium ion beam with a 75° incident angle, and the energy spectrums of emitted α particles were measured by an Au–Si surface barrier detector at the scattering angle of 30° in laboratory coordinate system. In addition, the composition of the film was determined by RBS with a 1.305 MeV proton ions beam perpendicular to the sample surface. The ERDA and RBS spectra were transformed into depths profiles using the SIMNRA program.[25] Based on the RBS and ERDA measurements, the average atomic ratios of D/Zr and H/Zr at the near-surface layer ($\sim$ 0.3 μm) were obtained as presented in Table 1. And the results of the original sample were similar to those with an implantation fluence of 1×10^{16} protons/cm^2 and were not listed separately.

Table 1. The average atomic ratios of D/Zr and H/Zr were obtained by ERDA at the near-surface layer ($\sim$ 0.3 μm) on different implantation fluence.

Fluence (protons/cm^2)	D/Zr	H/Zr
1×10^{16}	1.51±0.06	0.0003±0.006
3×10^{16}	1.47±0.06	0.0003±0.006
1×10^{17}	1.48±0.06	0.015±0.007
1×10^{18}	1.41±0.06	0.064±0.007

To determine more accurate depth profiles of the film H, D and Zr concentrations at greater depths, ToF-SIMS measurements[26] were conducted with a ToF-SIMS V spectrometer (ION-TOF GmbH, Münster, Germany) equipped with a Bi liquid metal primary ion source. 30 keV Bi^+ beam with a current of 1.34 pA was used as the analyzing beam, which was rastered over a 50×50 μm area. In the negative ion

signal mode, for D and H in ZrD_x, 2 keV Cs^+ ions with a current of about 100 nA were applied because of its significant enhancement of negative ions yield. In addition, a time-of-flight detector was employed to measure the secondary ions from the surface and the data collection time is 5000 s. Additionally, in the positive ion signal mode, a 2 keV O_2^+ ions beam at a current of 400 nA spread across 300×300 μm^2 with the sputtering time of 1000–2000 s was performed to analyze the depth profile of metal ions. The chamber pressure was maintained at about 3.1×10^{-7} Pa during each acquisition. ION - TOF Surface Lab software (ION-TOF GmbH, Münster, Germany, version 6.0) was used to analyze the original data.

TOF-SIMS provides well-resolved concentration depth profiles, and the shortcomings of absolute quantification could be compensated by ERDA measurement. Therefore, the SIMS counts were multiplied by a correction factor of $N_{\mathrm{ERDA}}/N_{\mathrm{SIMS(50-300\ nm)}}$ to get the absolute H and D depth profiles. Here, SIMS counts at a depth range of 50–300 nm were chosen to avoid the H/D absorption peak at the surface.

The surface morphology of the film surface was observed by SEM/EDS. The XRD patterns of the ZrD_x samples before and after protons implantation were recorded using Cu $K\alpha$ line by D/max-2400 (Rigaku Corporation) with a grazing incidence angle of 1°, operating at 40 kV voltage and 40 mA current to obtain the phase structure features especially within the implanted surface of ZrD_x samples. And the XRD patterns were analyzed by MDI Jade 6.0.

3. Results and discussion

3.1. Depth profiles analysis

The depth profiles of H/Zr and D/Zr atomic ratios measured by a combination of SIMS and ERDA are shown in Fig. 2. A swift dip is found in the region of 0–50 nm, which is caused by surface absorption of H from the air and has no relation to the proton implantation. It can be seen from Fig. 2(a) that the atomic ratio of H/Zr increases with proton fluence. At the lower fluence, it indicates that hydrogen distributes homogeneously throughout the thickness of the ZrD_x thin film. For fluence in the range from 1×10^{17} protons/cm^2 to 1×10^{18} protons/cm^2, a slight decrease of the H/Zr atomic ratio is found in the range of about 600–750 nm. In addition, two flat H/Zr depth profiles can be observed, and the crucial change happens to 600–750 nm. This is less than the implanted range simulated by SRIM software as shown in Fig. 1. The difference is mainly ascribed to the fact that the SRIM code does not consider the H atoms diffusion in lattice or be trapped by defects. Some implanted protons are trapped in defect areas induced by proton irradiation and forms the higher profile region, which grows up and shifts to deeper with the implantation fluence. While many H atoms cannot be trapped and stay at interstitial positions temporarily, and then would diffuse to a low concentration zone driven by concentration gradient in the full film according to Fick's law,[27,28] which is consistent with the previous investigations.[29–31]

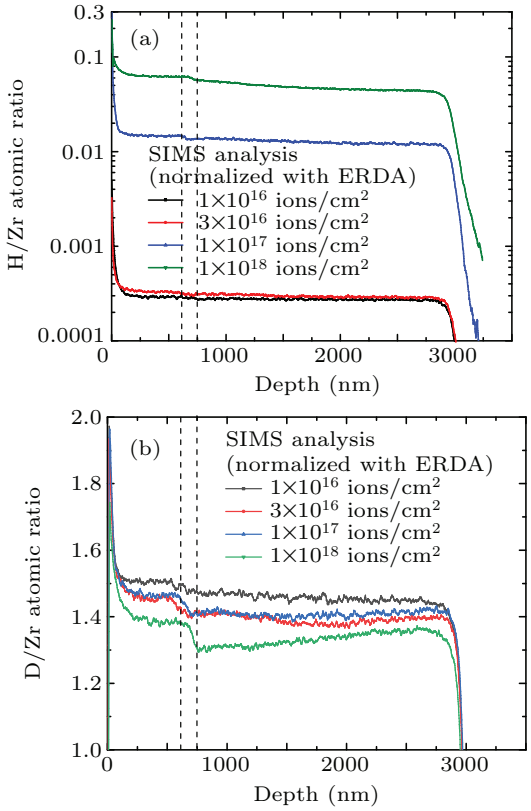


Fig. 2. Depth profiles of H/Zr (a) and D/Zr (b) by SIMS normalized with ERDA at various implantation fluence.

In addition, as shown in Fig. 2(b), the atomic ratio of D/Zr decreases with proton irradiation, which is caused by both forming of zirconium hydride and the release of free D by diffusion. A sharp decline appears at about 600–750 nm, which corresponds to the severe irradiation damage region (Fig. 1). It can be explained by the decomposition of deuteride (Zr-D_x) and the decrease of the D/Zr ratio caused by proton damage at the end range. For these values of deuterium concentration here, the α and γ phases are guessed to form, where the D (H) atoms are in the quasi-free and semi-stable state, respectively.[32,33] Thus, resulting in the D (H) atoms are easy to diffuse and deuteride (hydrides) is not easy to recombine in this region.

It is evident that the H concentration increases, while the D concentration decreases in the whole ZrD_x film with proton fluence. Because D and H have the same chemical properties, the exchange between H and D atoms could happen in the whole film with some probability. Zr-H_x could be therefore formed in proton implanted ZrD_x film. But inside of the proton range, Zr-D_x decomposition was caused by irradiation, and the exchange probability was significantly enhanced due to the free Zr recombines with H. This similar replacement

phenomenon of hydrogen isotopes has also been demonstrated by Doyle.[16] Consequently, it is confirmed there was obvious replacement behavior in the ZrD_x film during protons implantation from the depth profile.

3.2. Model of isotopic replacement behavior

In order to further investigate the replacement behavior of hydrogen isotopes with the increase of proton fluence, the atomic ratios of H/Zr and D/Zr in the range of 0.3–0.5 μm are averaged. This range is determined to avoid the influence of surface effects and irradiation damage. For the depth deeper than 0.6 μm, as shown in Fig. 2(b), a dramatic decrease of the D/Zr ratio occurs because of severe damage indicated in Fig. 1 (SRIM). The experimental values of average atomic ratios of D/Zr and H/Zr as functions of proton fluence are presented in Fig. 3, in which the H/Zr is multiplied by 10 to show the data more clearly. Obviously, an increase of the proton fluence from 1×10^{16} to 1×10^{18} ions/cm^2 leads to an increase of H/Zr from 0 to 0.0626, whereas the D/Zr decreases from 1.51±0.06 to 1.39±0.06, with a total decline of D/Zr about 0.12.

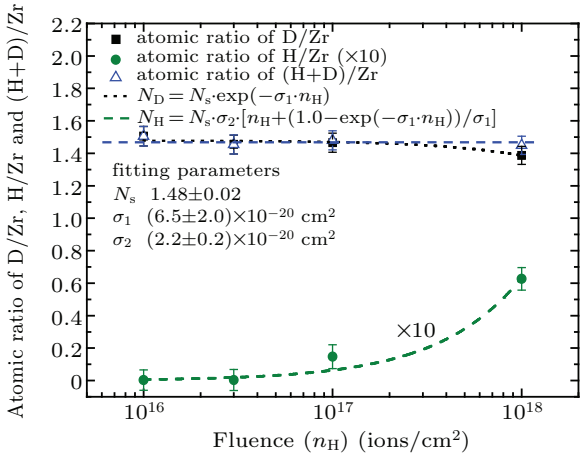


Fig. 3. The proton fluence dependence of the average atomic ratio of D/Zr, H/Zr and (H+D)/Zr in the surface layer (0.3–0.5 μm) of ZrD_x film. The dotted and dashed lines are theoretical fitting of retained D/Zr and H/Zr atomic ratios.

In previous work, Hughey indicated that the loss of tritium away from range-end can be attributed to beam enhanced detrapping of tritium from its bound sites and subsequent refilling of the vacant sites with implanted deuterons.[11] In Blewer and Doyle's works,[16–18] a decay model $N_D = N_s \cdot \exp(-\sigma \cdot n_H)$ was explicitly proposed to explain the deuterium amount remaining in the lattice after a proton fluence n_H. According to these models, we assume

$$\frac{dN_D}{dn_H} = -\sigma_1 N_D, \tag{1}$$

where N_D is the D/Zr ratio at proton fluence n_H, and σ_1 is the deuterium detrapping cross-section, which describes the deuterium detrapping probability when irradiated by protons. This leads to a solution as following:

$$N_D = N_s e^{-\sigma_1 n_H}, \tag{2}$$

where N_s is saturated D/Zr ratio before proton implantation. This fact (Fig. 3) indicates that the decay equation reproduces excellently the experimental results.

For the H/Zr ratio, Doyler *et al.*[16] assumed that additional hydrogen coming to the rest in the saturated region would find available trapping sites when the previously trapped deuterium is detrapped, and free atoms which could not be trapped would escape from the target surface. And they believed that the summation of two types of hydrogen isotopes should be constant at the saturated region, i.e., $N_D + N_H = N_s$, which leads to $dN_H/dn_H = -dN_D/dn_H$ and is different from the result observed in this experiment. In our work, the number density of trapping sites $\sim 0.12N_{Zr}$ (N_{Zr} is the atomic density of Zr in ZrD_x film) is obtained through the detrapping process induced by proton irradiation at maximum proton fluence of 1.0×10^{18} ions/cm^2. However, only $\sim 0.06N_{Zr}$ sites are occupied by incoming proton. This difference at high ion fluence may result from structure modifications caused by ion irradiation. As the protons fluence increased, the concentration of gas-filled voids within the sub-surface layer increases, and interconnected porosity starts to develop after certain fluence.[12] This leads to the recombination and release of a fraction of the molecular hydrogen. Therefore, according to our experiment results, the amount of retained protons is described separately by Eq. (3) as follows:

$$\frac{dN_H}{dn_H} = -\sigma_2 (N_s - N_D), \tag{3}$$

which means the increase of H/Zr ratio per unit flux of protons is proportional to the available trapping sites ($N_s - N_D$), where σ_2 is defined as trapping cross-section of the proton by trapping sites. Combining Eqs. (2) and (3), we get

$$N_H = N_s \cdot \sigma_2 \left[n_H + \frac{1}{\sigma_1} \left(1 - e^{-\sigma_1 n_H} \right) \right]. \tag{4}$$

Equations (2) and (4) give the variation behavior of D/Zr ratio and H/Zr ratio with an increase of proton fluence. As shown in Fig. 3, the trends of D/Zr and H/Zr ratio with the increase of proton fluence are described reasonably by this model for the isotopic replacement process in our experimental conditions. Here, the number density of saturated trapping sites N_s is 1.48±0.02 N_{Zr}. For the best fitting, and deuterium detrapping cross-section σ_1 and trapping cross-section of the proton by trapping sites σ_2 are determined to be (6.5±2.0)×10^{-20} cm^2 and (2.2±0.2)×10^{-20} cm^2, respectively.

It has been reported that the deuterium detrapping cross-section for D pre-implanted SiC with 5 keV H_2^+ is

2.6×10^{-18} cm^2, which is much larger than that for ZrD_x with 150 keV.[34] This is consistent with the trend that the replacement cross-sections decrease monotonically with increasing implant energy, which was illustrated by Blewer's work.[18] It is considered that the formation of more voids and vacancy clusters at high implant energy leads to the increase of free D atoms in recapture probability. It suggests that the implant energy is one of the factors in determining the amount of deuterium detrapping. The speculation also needs more fully test to investigate.

It could also be concluded that the deuterium detrapping process dominates the hydrogen isotope retention in target film because the deuterium detrapping cross-section σ_1 is 2–4 times of the trapping cross-section σ_2, which means more deuterium is detrapped, and only the half of available trapping sites are occupied by incoming proton. However, this phenomenon was not observed by Doyler and Blewer *et al.*[16,18] because the proton energy range in their work was 1–14 keV, which is lower than 150 keV used in our work. In our experiment, the target temperature was at room temperature, which was higher than $-120°$ applied in Blewer's work. Therefore, hydrogen atoms' mobility is increased in the experimental conditions of this work, and the enhanced mobility also means the higher escaping amount from the sample surface.[29] This also shows that the isotopic replacement phenomenon is dependent on the beam energy, target materials as well as the target temperature.

3.3. XRD analysis

The XRD patterns of ZrD_x specimens implanted with various proton fluences are shown in Fig. 4, the observed diffraction peaks at 32.24°, 36.00°, 52.09°, 54.84°, and 62.38° correspond to (111), (200), (220), (202), and (311) planes, respectively. It can be seen that no additional peaks were found in all the irradiated specimens, and (220) reflection peak has almost disappeared in the diffraction pattern when the proton fluence is 1×10^{18}. Taking into account the previous investigation,[22,31] it is reasonable to conclude that the low-energy particles irradiation does not lead to the generation of a new phase in ZrD_x, while partial lattice distortion may be caused by the introduction of defects at higher fluence. To further evaluate the microstructure effects of proton implantation in the injected region surface, the calculated crystallite size and microstrain along (111) are given in Table 2.[35,36] With ion fluence increasing from 1×10^{16} to 3×10^{16} protons/cm^2, the crystallite size increases slightly, but the crystallite size indicates a decreasing trend and microstrain rise by further increasing the proton fluence. However, there is little overall significant difference in values compared with the un-irradiated samples. And according to the previous studies,[22] such results are reasonable due to the limited irradiation effects of low energy protons on the microstructural property of zirconium alloy in implanted region.

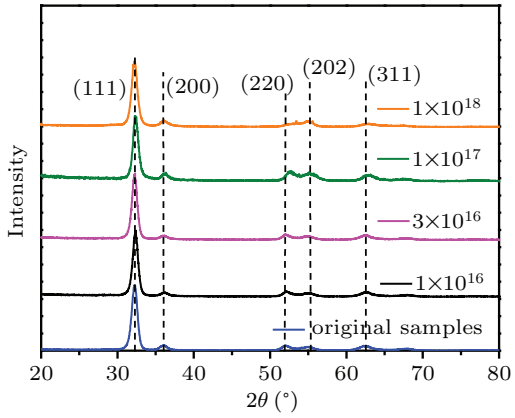


Fig. 4. The XRD patterns normalized of the ZrD_x samples before and after protons implantation.

Table 2. Structural parameters of (111) plane on various implantation fluence.

Implantation fluence (protons/cm^2)	2θ (°)	FWHM (°)	Crystallite size (nm)	Microstrain (10^{-2})
Original samples	32.24	0.873	9.812	1.04
1×10^{16}	32.22	0.827	10.327	0.94
3×10^{16}	32.24	0.757	11.331	0.78
1×10^{17}	32.30	0.812	10.701	0.87
1×10^{18}	32.22	0.884	9.665	1.07

3.4. Surface morphology

The surface morphologies of ZrD_x specimens implanted with different proton fluence are shown in Fig. 5. With the increase of protons fluence from 1×10^{16} to 1×10^{17}, there is no observable morphological difference in the implanted-proton specimens compared to the original, suggesting little mechanical damage due to the proton implantation. This is in agreement with the phenomenon observed in previous studies.[29,30] However, the circular flaking areas with a diameter of about 100 μm homogenously distribute in the ZrD_x surface are visible when the implantation fluence increases to 1×10^{18} proton/cm^2 (Fig. 5(e)). Compositional analysis of these circular flaking areas is carried out by using energy dispersive x-ray spectroscopy (EDS) presented in Fig. 5(e), and results confirm that the Si substrate (purple area) was completely exposed.

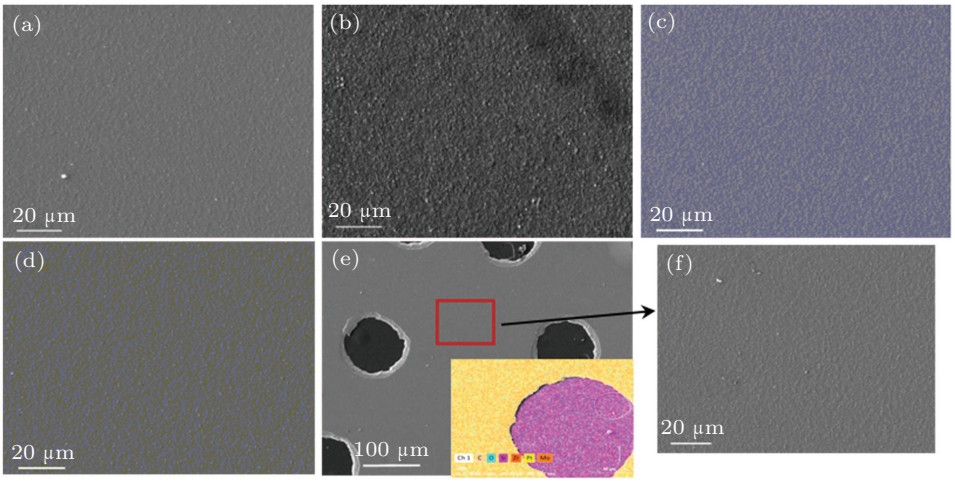


Fig. 5. SEM images of ZrD_x implanted protons at different dose, (a) without implantation, (b) 1×10^{16} protons/cm^2, (c) 3×10^{16} protons/cm^2, (d) 1×10^{17} protons/cm^2, (e) 1×10^{18} protons/cm^2 under different magnifications, and EDS analysis result was shown as insert in (e).

As mentioned in the previous section, the probability for H atoms trapped by defects in the implanted region is quite less, compared to the number of implanted protons. Most of the H atoms would diffuse to a deeper region, even to substrate at higher fluence, as can also be seen from the depth profiles of H in Fig. 2(a). It is noticed that the lattice size of Si crystal grain is 72.48% larger than that of Mo, which could contribute to forming a large amount of mismatch dislocation between the deposited material and the substrate during the growth of the Mo layer on the Si substrate's surface.[37,38] These H atoms tended to diffuse to these structures and be captured, which could lead the number of H atoms to congregate so that the H micro-bubbles nucleated at the interface. With increasing implantation fluence to 1×10^{18} protons/cm^2, the growing H clusters might eventually reach excessive compressive stress that the pressure disrupted the bubbles to release the H atoms inside, ending with the surface flaking area development. And the growth process of surface damage was similar to the previous results,[15] but in this study, the H atoms were accumulated at the substrate interface due to the intrinsic defects introduced in the preparation process of the target, rather than the defects induced by irradiation. Consequently, the creation of long-living targets requires the selection of suitable alternative substrate materials, such as Nb and Cu.

4. Conclusions

The influence of 150 keV protons implantation on the hydrogen isotopes replacement behavior and microstructure of ZrD_x film have been investigated with fluence range from 1×10^{16} to 1×10^{18} protons/cm^2. The D/Zr and H/Zr depth profiles were analyzed by ToF-SIMS combined with RBS and ERDA measurements. The depth profile results demonstrate that the H and D concentrations show a decline at 600–750 nm corresponding to the severe radiation damage region (SRIM). Furthermore, the D/Zr concentration decreases with increasing the proton fluence to 1×10^{18}. A modified model is established to analyze well the retention and decay curves of H and D in ZrD_x, which demonstrates the probability is approximately 2–4 times for detrapped deuterium than for H atoms trapped by defects in implanted region.

It is found that no new phase is detected in all irradiated specimens from XRD results and the (220) plane almost disappears when the proton fluence is 1×10^{18} protons/cm^2. Circular flaking zones with a diameter of about 100 μm on the ZrD_x surface are observed from SEM when protons fluence increases to 1×10^{18} protons/cm^2. And EDS results reveal that the Si substrate is exposed from circular flaking zones. The phenomenon may be ascribed to the increase of compressive stress excessive from induced by the H atoms congregation because of metal substrate mismatch dislocation at the interface. This degradation on the film surface could generate a decrease in the performance of the neutron production target. Attention should be paid to the microscale property of suitable substrate materials for a long-living target.

References

[1] Klix A, Eichin R, Forrest R A, *et al.* 2007 *Fusion Eng. Des.* **82** 2558
[2] Ohnishi S, Kondo K, Azuma T, Sato S, Ochiai K, Takakura K, Murata I and Konno C 2012 *Fusion Eng. Des.* **87** 695
[3] Jakhar S, Abhangi M, Rao C V S, Basu T K, Bhade S P D and Reddy P J 2012 *Fusion Eng. Des.* **87** 184
[4] Monnin C, Bach P, Tulle P A, van Rompay M and Ballanger A 2002 *Nucl. Instrum. Meth A.* **480** 214
[5] Ludewigt B A, Wells R P and Reijonen J 2007 *Nucl. Instrum. Meth B.* **261** 830
[6] Terrani K A, Balooch M, Wongsawaeng D, Jaiyen S and Olander D R 2010 *J. Nucl. Mater.* **397** 61
[7] Wipf H, Kappesser B and Werner R 2000 *J. Alloys Compd.* **310** 190
[8] Uno M, Yamada K, Maruyama T, Muta H and Yamanaka S 2004 *J. Alloys Compd.* **366** 101
[9] Long X, Huang G, Peng S, Liang J and Yang B 2011 *Nucl. Sci & Eng.* **60** 1568
[10] Čufar A, Batistoni P, Ghani Z, Giacomelli L, Lengar I, Loreti S, Milocco A, Popovichev S, Pillon M, Rigamonti D, Rebai M, Tardocchi M and Snoj L 2018 *Fusion Eng. Des.* **136** 1089
[11] Hughey B J 1995 *Nucl. Instrum. Meth B* **95** 393

[12] Alimov V K, Roth J and Lindig S 2008 *J. Nucl. Mater.* **381** 267
[13] Tang X H, Shi L Q, O'Connor D J and King B 2014 *J. Nucl. Mater.* **446** 200
[14] Monnin C, Ballanger A, Sciora E, Steinbrunn A, Alexandre P and Pelcot G 2000 *Nucl. Instrum. Meth A* **453** 493
[15] Anzorena M S, Bertolo A A, Gagetti L, Gaviola P A, Del Grosso M F and Kreiner A J 2018 *Appl. Surf. Sci.* **433** 68
[16] Doyle B L, Wampler W R, Brice D K and Picraux S T 1980 *J. Nucl. Mater.* **93** 551
[17] Doyle B L, Brice D K and Wampler W R 1981 *Radiat. Eff. Defect. S* **57** 81
[18] Blewer R S, Behrisch R, Scherzer B M U and Schulz R 1978 *J. Nucl. Mater.* **76** 305
[19] Karamanis D 2002 *Nucl. Instrum. Meth B* **195** 350
[20] Fournier L, Serres A, Auzoux Q, Leboulch D and Was G S 2009 *J. Nucl. Mater.* **384** 38
[21] Wang B Y, Xiang W, Dai J Y, Tan X H, Cheng L, Chen L and Qin X B 2011 *Acta Phys. Sin.* **60** 042902 (in Chinese)
[22] Liu Y, Xiang W, Zhang G and Wang B 2013 *Appl. Surf. Sci.* **285** 557
[23] Astrelin V T, Burdakov A V, Bykov P V, Ivanov I A, Ivanov A A, Jongen Y, Konstantinov S G, Kudryavtsev A M, Kuklin K N and Mekler K I 2010 *J. Nucl. Mater.* **396** 43
[24] Suarez Anzorena M, Bertolo A A, Gagetti L, Gaviola P A, del Grosso M F and Kreiner A J 2018 *Appl. Surf. Sci.* **443** 68
[25] Mayer M 1999 *AIP Conference Proceedings* **475** 541
[26] Mändl S, Bohne Y, Gerlach J W, Assmann W and Rauschenbach B 2006 *Nucl. Instrum. Meth B* **249** 297
[27] Ryabtsev S, Gasparyan Y, Zibrov M, Shubina A and Pisarev A 2016 *Nucl. Instrum. Meth B* **382** 101
[28] Waisman J L, Sines G and Robinson L B 1973 *Metal. Mater. Trans. B* **4** 291
[29] Hai L, Zhang H, Dong S, Xiao J and Zhang Z 2013 *ASSP* **32** 417
[30] Wang T, Long J, Wang S, Yang Z, Li J, Huang G, Zhang L, Jian Yang A and Renshaw Wang X 2017 *Sci. Rep.* **7** 13304
[31] Liang J, Peng S, Long X, Zhang X and Zhang T 2003 *Journal of Isotopes* **16** 151
[32] Chen M, Peng S, Zhou X, Long X and Fu Y 2016 *Chin. J. Rare Metals.* **40** 727
[33] Wang T S, Lv H Y, Grambole D, Yang Z, Peng H B and Han Y C 2009 *J. Nucl. Mater.* **386** 214
[34] Oya Y, Suzuki H, Morita K, Iinuma K, Uchida S, Makide Y and Tanaka S 2002 *Fusion Eng. Des.* **61** 705
[35] Kungumadevi L, Rajasekar K, Subbarayan A and Sathyamoorthy R 2008 *Ionics* **14** 63
[36] Ahmed A, Afzal N, Devarajan M and Subramani S 2016 *Materials Res. Express* **3** 116405
[37] Albrecht M, Christiansen S, Michler J, Dorsch W, Strunk H, Hansson P and Bauser E 1995 *Appl. Phys. Lett.* **67** 1232
[38] Peng C S, Li Y K, Huang Q and Zhou J M 2001 *J. Cryst. Growth.* **227** 740